

Published in final edited form as:

*Neuroimage*. 2013 August 15; 77: 195–206. doi:10.1016/j.neuroimage.2013.03.056.

## Fiber tract-driven topographical mapping (FTTM) reveals microstructural relevance for interhemispheric visuomotor function in the aging brain

Tilman Schulte<sup>a,\*</sup>, Mahnaz Maddah<sup>a</sup>, Eva M. Müller-Oehring<sup>a,b</sup>, Torsten Rohlfing<sup>a</sup>, Adolf Pfefferbaum<sup>a,b</sup>, and Edith V. Sullivan<sup>b</sup>

Tilman Schulte: tilman.schulte@sri.com

<sup>a</sup>SRI International, Neuroscience Program, 333 Ravenswood Ave, Menlo Park, CA 94025, USA

<sup>b</sup>Department of Psychiatry and Behavioral Sciences, Stanford University, Stanford, CA 94305, USA

### Abstract

We present a novel approach – DTI-based fiber tract-driven topographical mapping (FTTM) – to map and measure the influence of age on the integrity of interhemispheric fibers and challenge their selective functions with measures of interhemispheric integration of lateralized information. This approach enabled identification of spatially specific topographical maps of scalar diffusion measures and their relation to measures of visuomotor performance. Relative to younger adults, older adults showed lower fiber integrity indices in anterior than posterior callosal fibers. FTTM analysis identified a dissociation in the microstructural – function associates between age groups: in younger adults, genu fiber integrity correlated with interhemispheric transfer time, whereas in older adults, body fiber integrity was correlated with interhemispheric transfer time with topographical specificity along left-lateralized callosal fiber trajectories. Neural co-activation from redundant targets was evidenced by fMRI-derived bilateral extrastriate cortex activation in both groups, and a group difference emerged for a pontine activation cluster that was differently modulated by response hand in older than younger adults. Bilateral processing advantages in older but not younger adults further correlated with fiber integrity in transverse pontine fibers that branch into the right cerebellar cortex, thereby supporting a role for the pons in interhemispheric facilitation. In conclusion, in the face of compromised anterior callosal fibers, older adults appear to use alternative pathways to accomplish visuomotor interhemispheric information transfer and integration for lateralized processing. This shift from youthful associations may indicate recruitment of compensatory mechanisms involving medial corpus callosum fibers and subcortical pathways.

### Keywords

Interhemispheric function; Diffusion tensor imaging; Fiber tract-driven topographical mapping; FTTM; Corpus callosum; Pons; Aging

## Introduction

Efficient perception of multiple objects in a scene depends on complex visual processes of interhemispheric integration enabled by the microstructural and functional integrity of the corpus callosum (CC) (Genç et al., 2011; Gooijers et al., 2011; Schulte et al., 2010). Studies using diffusion tensor imaging (DTI) have established that the CC undergoes a variety of degenerative changes with normal aging, especially of myelinated fibers of the anterior relative to posterior callosal sectors (Lu et al., 2012; Madden et al., 2009; O'Sullivan et al., 2001; Sullivan et al., 2010). A fundamental challenge is in determination of the functional relevance of regional callosal fiber bundles for interhemispheric integration and transfer and whether age-related microstructural degradation of anterior callosal regions slows interhemispheric visuomotor processing and decreases transcallosal inhibition (de Chastelaine et al., 2011; Linnert and Roser, 2012). Recent neuroimaging studies provide some evidence that degradation of cross-hemispheric fiber integrity in older adults can compromise the efficiency of sensorimotor transfer required for visual bihemispheric integration (Davis et al., 2012; Douaud et al., 2011; Madden et al., 2004). Conversely, greater bilateral cortical cooperation for bimanual integration in older adults can be enabled by greater callosal tract microstructural integrity (Fling and Seidler, 2011).

The crossed–uncrossed difference (CUD) and redundant targets effects (RTE) tasks represent two distinct behavioral paradigms commonly used to probe functions of interhemispheric transfer and integration in humans. Both are simple reaction time (RT) tasks with lateralized light flashes presented in the left or right visual hemifield. The RTE paradigm (Corballis, 2002) is used to study how the left and right cerebral hemisphere communicate to enhance performance beyond the processing capacities of a single hemisphere (Marks and Hellige, 2003) by comparing paired with single targets presented to one or both visual hemifields (for a review, see Schulte and Müller-Oehring, 2010). Typically, responses are faster to stimulus pairs than single stimuli (Iacoboni and Zaidel, 2003; Miller, 1986; Mordkoff and Yantis, 1991; Roser and Corballis, 2003; Savazzi and Marzi, 2004; Schulte et al., 2004, 2005) with performance advantages from bilateral redundant targets indicating hemispheric resource sharing to make this redundant targets process more efficient (Maertens and Pollmann, 2005).

Two theoretical explanations can account for redundancy gains from paired stimulation, the 'horse race' model (Raab, 1962) and the 'co-activation' model (Miller, 1982). The 'horse race' model assumes that each stimulus is transmitted along separate channels and the response is triggered as soon as a decision is made by either one of the two channels (Mordkoff and Yantis, 1991). However, co-activation from otherwise independent processing channels may occur to increase signal strength of redundant targets (Miller, 1982; Reuter-Lorenz et al., 1995; for a review, Schulte and Müller-Oehring, 2010). Co-activation has been inferred from statistical facilitation, i.e., when facilitation from bilateral redundant targets exceeded probability predictions (Raab, 1962). However, with the rise of neuroimaging techniques, Miller's theoretical term co-activation has been expanded to neural interaction models (Corballis, 2002). At this point, functional neuroimaging studies in adults indicate that extrastriate visual pathways are selective for integration of visual targets (Schulte et al., 2006, 2010).

However, in healthy subjects, considerable inter-subject variability for RTE has been observed (Corballis, 2002) implying that different neural mechanisms are involved in interhemispheric visuomotor integration depending on strategy selection, task demands, and stimulus characteristics (Schulte et al., 2006). Accordingly, the facilitation effect has been attributed to co-activation at the sensory, cognitive, or motor processing stage (Mooshagian et al., 2009; Pollmann and Zaidel, 1999; Schulte et al., 2006). In addition, age contributes to

inter-subject variability in RTEs; some recent evidence indicates that the bilateral RTE is increased in older individuals (Linnet and Roser, 2012) and that subtle disruptions of callosal integrity can contribute to enhanced RTEs (Schulte et al., 2005).

In the CUD paradigm (Poffenberger, 1912), the interhemispheric transfer time is measured behaviorally by presenting targets in the same (uncrossed) or opposite (crossed) visual field in relation to the responding hand (Poffenberger, 1912; Zaidel and Iacoboni, 2003). The difference in reaction times between crossed and uncrossed conditions (i.e., the crossed-uncrossed difference, CUD) serves as an index of callosal interhemispheric transfer time, based on the assumption that uncrossed responses can be processed within the same hemisphere, whereas crossed responses require transfer of visuomotor information between hemispheres via the CC (Mooshagian et al., 2009; Poffenberger, 1912; Schulte and Müller-Oehring, 2010). Several studies indicate that the CUD is affected in older adults (Jeeves and Moes, 1996; Reuter-Lorenz and Stanczak, 2000; Schulte et al., 2004). Although not all studies could find an increase in the magnitude of the CUD in older adults (Hoptman et al., 1996), recent DTI studies have revealed correlations between subtle variations in regional white matter callosal microstructure and behavioral measures of interhemispheric transfer time and cognitive ability (Muetzel et al., 2008; Sullivan et al., 2010; Wolf et al., 2012). Fractional anisotropy (FA), an index of white matter fiber integrity, of anterior callosal regions is lower than in posterior regions and typically decreases disproportionately with advancing age (region of interest analyses: Pfefferbaum and Sullivan, 2003; Pfefferbaum et al., 2000, 2005; Salat et al., 2005; fiber tracking analyses: Stadlbauer et al., 2008; Sullivan et al., 2006, 2010; Zahr et al., 2009; stereology in postmortem human brains: Hou and Pakkenberg, 2011). Low FA in callosal genu and splenium correlated with longer interhemispheric transfer time measured with the CUD indicating that disruption of CC microstructure in normal aging is associated with declines in interhemispheric transfer (Schulte et al., 2005). Thus, age-related alterations in the CUD measure of interhemispheric transfer time could be due to degradation of both anterior and posterior callosal routes (Fling et al., 2011).

RTE and CUD are behavioral measures of interhemispheric function, each indexing a different neural mechanism. In theory, Iacoboni et al. (2000) assumed that the brain's loci of interhemispheric transfer and integration are reflected in CUD relative to RTE measures. For example, patients with resection of the corpus callosum showed a marked lengthening of the CUD due to the use of relatively inefficient ipsilateral pathways in making crossed responses (Marzi et al., 1991, 1999). However, these split-brain patients paradoxically demonstrated an enhanced RTE, i.e., an improved facilitation from paired stimulation, which has been attributed to cortical projections to a subcortical arousal system normally inhibited by the CC (Corballis, 2002; Savazzi and Marzi, 2004).

Here, we studied the role of age-related subtle degradation of interhemispheric microstructure for interhemispheric transfer and integration. Until now, a fine-grained anatomical mapping has not been available to test specific patterns of microstructural integrity and functional variability of interhemispheric integration in aging (Linnet and Roser, 2012). Thus, the fundamental goal is to identify specific fiber pathways that subserve selective processes of these interhemispheric skills. To test the relationship between bilateral processing advantages (RTE) and interhemispheric transfer time (CUD) we applied a recently developed, novel analysis approach, fiber tract-driven topographical mapping (FTTM), to pinpoint age-related differences of regional fiber integrity in relation to interhemispheric function. With this method, we previously demonstrated that age-related differences in fiber integrity are not uniform but rather locally specific along fiber trajectories (Maddah et al., 2011). Thus, spatially-specific alterations in microstructure of

CC and pons in healthy aging may selectively contribute to inter-subject variability in CUD and RTE measures.

We tested the hypothesis that, compared with younger individuals, older individuals would exhibit higher CUD that would be related to FA in anterior but not posterior regions of the CC; and that older adults would show a greater RTE that would be mediated by subcortical pontine fiber pathways, which are robust to aging (Stadlbauer et al., 2008; Sullivan et al., 2010), providing an alternative route for neural interhemispheric facilitation. In addition, FTTM-derived brain structural connectivity was validated with conventional tract-based spatial statistics (TBSS) analysis, and the neural co-activation assumption for RTE was tested with task-activated functional magnetic resonance imaging (fMRI). Based on our previous fMRI studies on RTE (Schulte et al., 2006, 2010), we hypothesized that RTE, i.e., paired > single stimulation, would elicit bilateral extrastriate activation, and that older age would modulate RTE-related activity at a subcortical processing level.

## Material and methods

### Participants

The participants were 21 younger (age range 19–30 years) and 16 older (age range 60–85 years) healthy adults (Table 1). Younger and older adults did not differ in sex distribution (younger: 10 women, 11 men; older: 7 women, 9 men). All subjects underwent clinical and neurological screening; none had a history of head trauma, documented compound skull fracture, clear neurologic sequelae, or any disease with potential central nervous system involvement, such as stroke, multiple sclerosis, or epilepsy. Three of the older subjects had diagnosed hypertension that was medically treated, and in-lab blood pressure measurements were within the normal range. One older participant had been diagnosed with type-2 diabetes 10 months prior to the study. All participants were right handed, spoke English as their first language, and had no history of illicit substance or alcohol abuse or dependence according to clinical interview using DSM-IV criteria. Both groups were highly educated (younger:  $16 \pm 1.2$  years; older:  $17 \pm 2.4$  years). Socioeconomic status (SES), determined using a 2-factor scale including both education and lifetime occupation (Hollingshead and Redlich, 1958), was insignificantly higher in the older than younger group. Relative to the younger group, the older group had higher estimated IQ scores (Table 1) based on the American National Adult Reading Test (ANART, Nelson, 1982). Subjects gave written informed consent to participate in this study, which was approved by the Institutional Review Boards at Stanford University School of Medicine and SRI International.

### Redundant targets task

A detailed description of the task was published previously (Schulte et al., 2010). In short, the task was to respond as quickly as possible to light flashes occurring for 150 ms in the left or right visual hemifield, regardless of whether the flashes appeared singly or in pairs. Stimuli were white disks on a dark, gray background, placed left or right of the fixation point and above the horizontal meridian. The inter-stimulus interval was randomly selected as 500, 700, or 900 ms. Throughout the test, subjects fixated on a point in the center of the display; to control fixation, subjects were also required to respond whenever they detected a flicker of the fixation point color from green to equiluminant yellow, which is detectable only within approximately  $1^\circ$  visual angle from the fixation point and was presented 40 times during the task.

Two task runs were presented, one requiring left-hand and one requiring right-hand responses, balanced across subjects. In total, 320 trials were presented, and each run comprised 160 trials. Behavioral responses were measured as reaction time (RT) to visual

field (VF) stimulation for left and right response hands. Differences in RT between crossed and uncrossed conditions, i.e., the crossed–uncrossed difference (CUD), indexed interhemispheric transfer time (crossed: left VF stimulus – right hand response, right VF stimulus – left hand response; uncrossed: left VF stimulus – left hand response, right VF stimulus – right hand response) (Poffenberger, 1912). The CUD formula is:  $CUD = RT_{crossed} - RT_{uncrossed}$ . Subtracting the sum of crossed responses from the sum of uncrossed responses and dividing this difference by two yielded the CUD (Fig. 3A).

The redundant targets effect (RTE) is considered to measure response facilitation from redundant (paired) stimulation (Miller, 1986; Mordkoff and Yantis, 1991; Roser and Corballis, 2003). Differences in RT between single and paired VF stimulation calculated the redundant targets effects (RTE), an index of visuomotor integration, where responses occur faster to paired than single stimuli. The RTE formula is  $RTE = RT_{S1S2} - (RT_{S1} + RT_{S2})/2$ , where S1S2 is two stimuli presented simultaneously as a pair, and S1 and S2 two stimuli presented singly (Fig. 4A). Thus, reaction time differences in RTE reflect the individual's overall response facilitation from redundant targets in milliseconds.

### DTI, MRI, and fMRI acquisition

Structural, diffusion, and functional imaging protocols were conducted on a clinical whole-body 3 T scanner (General Electric, Milwaukee, Wisconsin) with 8-channel head coil. Subject motion was minimized by following best practices for head fixation, and image series were inspected for residual motion. Scanning parameters for DTI were as follows: 2D echo-planar; axial acquisition; TR = 7300 ms; TE = 86.6 ms; thickness = 2.5 mm; skip = 0 mm; locations = 62; b = 0 [5 number of excitations (NEX)] + 15 noncollinear diffusion directions, b = 860 s/mm<sup>2</sup> (2 NEX) + 15 opposite-polarity noncollinear diffusion directions, b = 860 s/mm<sup>2</sup> (2 NEX); FOV = 240 mm; x-dim = 96, y-dim = 96; reconstructed to 128 × 128, 4030 total images. Two structural series were also acquired: a dual echo 2D-FSE, and a T1-weighted 3D-SPGR. The dual-echo FSE sequence (TR = 7850 ms, TE = 17/102 ms, thickness = 2.5 mm, skip = 0 mm, locations = 62) was at identical slice locations as the DTI and was used for co-registering structural and diffusion images as well as skull stripping. The T1-weighted SPGR (3D axial IR-prep-TR = 6.5 ms, TE = 1.6 ms, thick = 1.25 mm, skip = 0 mm, locations = 124) was used for tissue segmentation and region-of-interest parcellation. A field map for correction of spatial distortions in the diffusion-weighted images was generated from a gradient-recalled echo sequence pair (TR = 460 ms, TE = 3/5 ms, thickness = 2.5 mm, skip = 0 mm, locations = 62).

Scanning parameters for fMRI were as follows (Schulte et al., 2010): Whole-brain fMRI data were acquired with a T2\*-weighted gradient echo planar pulse sequence (2D axial, TE = 30 ms; TR = 2200 ms; flip angle = 90°; in plane resolution = 3.75 mm; thick = 5 mm; skip = 0 mm; locations = 36; FOV = 240 mm; 1 NEX). The start of the scan was triggered automatically from PsyScope software. Test instructions were reviewed with the subject by the examiner via the scanner's intercom system before the onset of each run. A dual-echo FSE (2D axial; TR = 5000 ms; TE = 17/102 ms; thick = 5 mm; skip = 0 mm; xy matrix = 256; flip angle = 90°; locations = 36; FOV = 240 mm; 1 NEX) was used for spatially registering the fMRI data.

### DTI processing

DTI quantification was preceded by eddy current correction on a slice-by-slice basis using within-slice registration. The diffusion effect created by the imaging gradients was corrected by taking advantage of the symmetry of the opposing-polarity acquisition (Neeman et al., 1991), reducing the data to 15 non-collinear diffusion-weighted images per slice for tensor computation. Using the field maps, B0-field inhomogeneity-induced geometric distortion in

the eddy current-corrected images (Bodammer et al., 2004) was corrected with PRELUDE (Phase Region Expanding Labeller for Unwrapping Discrete Estimates) and FUGUE (FMRIB's Utility for Geometrically Unwarping EPIs) (Jenkinson, 2003). From distortion-corrected diffusion-weighted images, tensors were estimated using the Teem library (<http://teem.sourceforge.net/>). From these tensors, scalar diffusion measures, including fractional anisotropy (FA), were also calculated on a voxel-by-voxel basis.

### Tract-based spatial statistics (TBSS)

FA images in native subject DTI space were analyzed using the TBSS method (Smith et al., 2006). To enable comparison between the two DTI analysis methods, the FA images were derived from the exact same tensor data for TBSS and FTTM. We followed the default TBSS procedure ([www.fmrib.ox.ac.uk/fsl/tbss/index.html](http://www.fmrib.ox.ac.uk/fsl/tbss/index.html)) to 1) align all images with the “JHU-ICBM-FA-1 mm” template included with FSL (the same template was also used for FTTM), 2) create and skeletonize a group-mean FA image, and 3) project all subject FA images onto the mean skeleton. The projected FA data from all individual subjects were then read into SPM for pixel-wise hypothesis testing. For group comparison, statistical thresholds were set at  $p_{\text{FWE corrected}} = 0.05$ .

### Fiber tract-driven topographical mapping (FTTM)

The linear organization of white matter fibers, an index of tissue quality, is detectable with diffusion tensor imaging (DTI) (Pierpaoli and Basser, 1996) and expressed as high fractional anisotropy (FA) of diffusion (Jones, 2010). Despite the microstructural detail and anatomical course revealed by DTI, quantification methods, especially tractography, are limited by their spatial resolution, reporting for example a single FA value per region of interest or fiber bundle. Region-of-interest analysis is particularly susceptible to contamination from partial voluming of crossing fibers. To overcome these shortcomings, FTTM (Maddah et al., 2008, 2011) takes advantage of fiber tract-driven geometric models to generate spatially and orientationally specific, tract-driven topographic maps of diffusion measures, thereby minimizing partial volume effects from crossing fibers.

For each subject, we tracked CC and pons fibers using streamline fiber tracking, mapped them to a common atlas space via linear image registration, and clustered fibers into bundles by applying a method based on an expectation maximization formulation (Maddah et al., 2008). This method permits probabilistic assignment of fiber streamlines to larger tract bundles and also provides a consistent parameterization along the length of each fiber in each bundle by establishing subject-to-model-to-subject point correspondences, thus enabling spatially-specific statistics over the entire extent of each bundle. Each tract model is derived from the cluster center (Maddah et al., 2008, 2011) and therefore provides an across-subject reference coordinate system for quantification of diffusion measures at corresponding sample locations along the trajectories assigned to that tract. In broad terms, FTTM refines quantification and visualization of diffusion-based fiber tracking using an expectation maximization formulation to create geometric consensus models for fiber bundles. Fig. 1 shows the pipeline of this DTI analysis.

A publicly available atlas of fiber tracts (ICBM-DTI-81; <http://www.loni.ucla.edu/ICBM/>) (Mori et al., 2008; but see Rohlfing, 2013) was used as a template, which is composed of a set of labeled regions, each corresponding to an anatomically-known bundle of fibers in the human brain. As the first step of the DTI analysis pipeline, the labeled regions in the atlas were mapped to each subject's native space to seed the tractography. To this end, pairwise affine registration, computed by using CMTK's “registration” tool (<http://nitrc.org/projects/cmtk/>), aligned the FA volume of each subject to the atlas. In the second step, streamline tractography for each subject, seeded from the mapped labeled atlas regions, was performed

in native subject DTI image space using 3D Slicer3 (<http://www.slicer.org>) (Fedorov et al., 2012). Fiber tracking used a step size of 0.5 mm and was terminated when an FA value less than 0.15 or maximum curvature of 0.8 (minimum cosine of the angle between current and next streamline segments) was encountered (Basser et al., 2000). During tracking, FA was computed at each point along the trajectories and stored for subsequent analysis. As the third step, after individual fiber tracking, trajectories from all 37 subjects were transformed back into the atlas space, via the previously computed atlas-to-subject image registrations. In the fourth step, the trajectories were clustered into tract bundles based on their spatial proximity and shape similarity to the medial representation of fiber tracts for the pons and three callosal regions (genu, body, splenium) in the ICBM DTI-81 atlas. A minimum-likelihood threshold of 0.2 was used in the EM clustering algorithm to reject outlier trajectories. To account for the respective shapes of tracts, the trajectories for the body of the CC were grouped as sheet-like bundles and clustered onto a medial surface, while the pons, genu, and splenium were grouped as tubular bundles and clustered onto a centerline. Note that the resulting models are two- and one-dimensional, respectively, i.e., the sheet-like bundles are mapped onto a surface that has no thickness, and the tubular bundles are mapped onto a line that has no radial extent. Thus, tubular tracts (such as pontine fibers) are represented by medial curves, whereas sheet-like tracts (such as the body of the CC) are represented by medial surfaces. The spatial distance between the most distant fibers assigned to that bundle, but not the medial model itself, determines the ultimate extent of each bundle perpendicular to the sheet or midline.

Finally, for each subject the mean FA was calculated for each point on the estimated medial representation of the bundle, based on the model-to-trajectory correspondences computed by the clustering algorithm. This procedure summarized the local variation of the diffusion parameter along each bundle in each subject as spatially-specific FA topography maps. The per-subject mean FA values at each tract model point were then used for hypothesis testing and statistical analysis. ANOVAs were used for statistical testing of group differences, and Pearson correlation was used for testing fiber FA correlations with behavioral measures, RTE and CUD. FDR-correction for height thresholds for statistics derived from neuroimaging data (Genovese et al., 2002), i.e., for each point correspondence in FTTM, requires a  $p < 0.012$  for the genu, splenium, and pontine ROIs, and a  $p < 0.0069$  for the callosal body ROI. Mean FA data for each ROI were extracted for each subject to plot RTE-FA and CUD-FA relationships. Significant Pearson correlations were confirmed with Spearman's *Rho* correlations.

### fMRI processing

Image preprocessing and statistical analyses were performed using the SPM8 software package (Wellcome Department of Cognitive Neurology). The fMRI analysis focused on the whole brain. The functional images were subjected to geometric distortion (field map) correction and motion correction. The FSE structural images were co-registered to the mean unwarped and motion-corrected functional image for each subject and segmented into gray and white matter images. Functional and structural gray matter images were normalized to Montreal Neurological Institute (MNI) space, and volumes were smoothed with a Gaussian kernel of 8 mm (FWHM). Individual statistics were computed using a general linear model approach (Friston et al., 1995a, 1995b) as implemented in SPM8. Statistical preprocessing consisted of high-pass filtering at 88 s, low-pass filtering through convolution with the canonical hemodynamic response function, and global scaling. A random-effects analysis was conducted for group averaging and population inference. One image per contrast was computed for each subject from a design matrix that included estimated individual movement parameters as regressors in addition to stimulation conditions as explanatory variables. RTE contrasts of interest were 'pair vs. sum of two single' stimulation and were

computed for left- and right-hand conditions. For second-level group analyses, these RTE contrast (pair > single) images were subjected to a factorial model involving 2 factors: Group (younger vs. older), and RTE (left hand vs. right hand). Analysis thresholds were set at  $p_{FWE\ corrected} < 0.05$  for combined spatial extent and peak intensity (Poline et al., 1997).

## Results

### Topographical mapping of callosal and pontine fiber FA

Based on spatially-specific statistics along each bundle, older adults had significantly lower FA values than younger adults at focal regions of the callosal genu, body, and splenium ( $p < 0.001$  is marked red, Fig. 2 lower panel). Topographical maps revealed lower FA in older than younger adults at nearly all locations of the midline genu fiber bundle. By contrast, lower FA in the older than younger adults was spatially specific in the body fiber sheet map and affected anterior fibers and lateral posterior fibers projecting towards left-hemispheric locations in premotor, somatosensory, and parietal cortices. In the callosal splenium, only the most medial regions differed significantly by group. FA differences in the pons were present only at focal bilateral locations ( $p < 0.001$  is marked red, Fig. 2).

We averaged FA over all points of the topographic map for each callosal ROI and entered the mean FA value for each bundle into a group-by-callosal sector ANOVA. Older adults had, on average, lower FA values than younger adults (group:  $F(1,35) = 53.25$ ,  $p < 0.0001$ ). FA was overall higher in the splenium than genu and body (callosal sector:  $F(1,35) = 80.8$ ,  $p < 0.0001$ ). Group differences, i.e., lower FA in older than younger adults, were more pronounced in anterior than posterior CC sectors (group-by-sector interaction:  $F(1,35) = 12.1$ ,  $p < 0.001$ ). Mean pontine fiber FA, averaged over all points of the topographic map, did not statistically differ between the age groups ( $t(35) = 1.54$ , *ns*).

To examine the convergence with widely used DTI quantification methods, we compared the FTTM results with TBSS results, with the caveat that the fundamentally different geometric representation of the results between FTTM (atlas-based medial model) vs. TBSS (image-based medial skeleton) makes it impossible to compare truly corresponding findings. Yet, TBSS-derived FA group results showed age group convergence with the principal FTTM-derived findings, including lower genu and body FA in older than younger adults, a focal region in the medial splenium and in the left-lateral pontine tract.

### Interhemispheric function: CUD and RTE

**Interhemispheric transfer (CUD)**—An ANOVA with group (younger, older) as the between-subject factor and CUD (crossed, uncrossed) and response hand (left, right) as the within-subject factors revealed that the groups did not differ in visuomotor interhemispheric transfer time (CUD) (group-by-CUD interaction:  $F(1,35) = 0.32$ , *ns*) (for similar findings, Linnet and Roser, 2012). Both groups showed significant CUDs for the nondominant (left) hand but not for dominant (right) hand responses (CUD-by-hand interaction:  $F(1,35) = 39.09$ ,  $p < 0.0001$ ) (Fig. 3A, Table 2).

**Interhemispheric integration (RTE)**—Despite descriptively larger RTEs in older (9 ms) than younger adults (2 ms), a group-by-RTE-by-hand ANOVA revealed that the facilitation from redundant targets did not differ statistically between the groups (group:  $F(1,35) = 1.31$ , *ns*; group-by-RTE-by-hand interaction:  $F(1,35) = 0.06$ , *ns*) (Fig. 4A, Table 2).

**Correlation between CUD and RTE**—Within-group analyses showed that longer interhemispheric transfer time (CUD) was modestly correlated with greater response facilitation from redundant targets (RTE) in older adults ( $Rho = 0.43$ ,  $p = 0.050$ ),

specifically for right-hand responses (RH:  $Rho = 0.45$ ,  $p = 0.039$ ; LH:  $Rho = 0.15$ ,  $ns$ ), but not in younger adults ( $Rho = 0.05$ ,  $ns$ ).

### Interhemispheric function and callosal and pontine fiber integrity

**CUD and local FA**—Correlating FTTM-derived FA values with CUD values for each group created spatially specific topographic correlation maps. In older adults, slower interhemispheric transfer of visuomotor information (larger CUDs) correlated with lower FA values in callosal body regions involving fibers projecting towards left-hemispheric premotor and supplementary motor regions and fibers connecting somatosensory regions between the two parietal lobes (Fig. 3B). In younger adults, no correlation in the callosal body reached statistical significance, but higher FA at medial locations in the genu fiber topographical map correlated moderately with smaller CUDs ( $p < 0.05$ ) (Fig. 3B).

For statistical testing of group differences in FTTM microstructure-function relationships, we extracted FTTM-derived FA values, calculated the average FA value for each ROI, and entered FA means into SPSS 20. Using CUD and FTTM-derived body FA mean values revealed an average Pearson correlation coefficient of  $r = -0.56$  ( $p = 0.012$ ;  $Rho = -0.66$ ,  $p = 0.003$ ) in older adults and  $r = 0.10$  ( $ns$ ;  $Rho = 0.08$ ,  $ns$ ) in younger adults. The average correlation coefficient between CUD and FTTM-derived genu FA mean values in younger adults was  $r = -0.47$  ( $p = 0.015$ ;  $Rho = -0.51$ ,  $p = 0.009$ ) and in older adults  $r = -0.16$  ( $ns$ ;  $Rho = -0.39$ ,  $p = 0.07$ ) (Fig. 3B). The correlation coefficients differed significantly between older and younger adults for CUD-body FA ( $z = -2.01$ ,  $p = 0.02$ ), but not for CUD-genu FA ( $z = 0.96$ ,  $ns$ ) ( $r$  to  $z_r$  transformation [ $z_r = 0.5 \log_e(1 + r)/(1 - r)$ ] (Walker and Lev, 1953)). In addition, convergence of FTTM results with TBSS-derived FA-CUD correlations was found for the callosal body in older adults ( $p = 0.005$ ) (Fig. 3C).

### Interhemispheric facilitation (RTE) and local FA

In older but not younger adults, RTE correlated highly with FA values in the anterior transverse pontine fibers that branch into the right cerebellar cortex (Fig. 4B). Using FTTM-derived mean FA values averaged over the right branch of the pontine bundle, within group correlation analysis (SPSS 20) revealed that higher mean pontine FA predicted greater bilateral processing advantages in older adults ( $r = 0.47$ ,  $p = 0.03$ ;  $Rho = 0.56$ ,  $p = 0.013$ ), but not younger adults ( $r = -0.14$ ,  $ns$ ;  $Rho = 0.03$ ,  $ns$ ). The correlation coefficients for RTE-pontine FA differed significantly between groups ( $z = 1.79$ ,  $p = 0.037$ ). TBSS-derived FA measures did not reveal pontine FA-RTE correlations in either group.

### Interhemispheric facilitation (RTE)-related BOLD activation

To test the neural correlate of redundancy gain, fMRI analysis compared whole brain activation during paired stimulation with that during single stimulation ( $S1S2 > S1 + S2$ ). Thus, the perceptual input is exactly the same for the paired ( $S1S2$ ) and the single condition ( $S1 + S2$ ). Brain activity derived from this contrast reflects activation to bilateral paired stimulation over and above the activation invoked by single stimuli in the left or right visual hemifield, and serves as a neural substrate for co-activation from redundant targets. As hypothesized, we found bilateral extrastriate activation for the RTE contrast. In addition, a group-by-RTE response hand interaction revealed more bilateral activity in older than younger adults in a pontine cluster involving the left superior colliculus, and extending to the left thalamus, and right superior cerebellum, for dominant right-hand responses (in contrast to left-hand responses) (Fig. 4c, Table 3). A second medial superior temporal cortex activation cluster, significant at  $p_{FDR\text{corr}} < 0.05$ , showed a similar interaction pattern (Table 3).

## Discussion

We studied the functional ramifications of focal callosal and pontine fiber integrity in the aging brain using fiber tract-driven topographical mapping (FTTM), enabling high spatial specificity of scalar diffusion maps (Maddah et al., 2011). Despite callosal fiber degradation in older compared with younger adults, neither the behavioral measure of interhemispheric transfer nor that of bilateral processing advantage was disturbed, but the locus of microstructure-function associates differed between age groups. In younger adults, normal variation in fiber integrity in the genu correlated with interhemispheric transfer times (CUD), whereas in older adults, fiber integrity in left lateral and medial regions of the callosal body was related to the CUD. In addition, robust pontine fiber integrity correlated with greater bilateral processing advantages (RTE) in older adults, supporting a role for the pons in facilitating neural interhemispheric information transfer. Here, fMRI provided convergent evidence for a cortico-subcortical involvement in interhemispheric facilitation. In addition to the hypothesized extrastriate cortical activation in older and younger adults, neural co-activation from redundant targets occurred in the pons and was modulated by age and response hand.

Thus, with compromise of anterior callosal fibers, older adults may have available intact medial fibers of the CC connecting premotor, motor, and somatosensory cortices and subcortical pontine pathways to accomplish visuomotor transfer and integration required for lateralized processes. Accordingly, interhemispheric transfer does not rely solely on the CC, but also draws on subcortical pathways that balance hemispheric activation according to task demands (Saltzberg et al., 1986; Schulte and Müller-Oehring, 2010; Teipel et al., 2009).

### Topographical mapping of white matter integrity in healthy aging

Studies on aging report compromise of the brain's white matter microstructure associated with a decline in sensorimotor and control functions (Bartzokis et al., 2004; Bennett et al., 2010; Madden et al., 2009; Marchand et al., 2011; Raz et al., 2010; Stadlbauer et al., 2008; Sullivan et al., 2010; Zahr et al., 2009). Application of FTTM enabled spatially specific investigation of the anatomical and functional relevance of interhemispheric transfer and bilateral facilitation in aging. Consistent with studies using fiber tracking in aging (Bennett et al., 2010; Stadlbauer et al., 2008; Sullivan et al., 2010; Zahr et al., 2009), we found that anterior callosal fibers were more vulnerable to age-related degradation than posterior ones, whereas pontine fiber integrity was robust to age. Age-related differences in callosal fiber integrity were not uniform but rather locally specific along fiber trajectories demonstrating, in addition to an anterior-posterior gradient, a left-to-right gradient in the vulnerability of body fibers.

Comparing FTTM with TBSS, a conventional white matter fiber tractbased analysis technique, we found consistency in the results, i.e., lower genu FA in older than younger adults (for TBSS-derived age-related fiber degradation, see also Bennett et al., 2010; Burzynska et al., 2010), despite fundamentally different approaches of these methods.

### Functional ramification of topographical mapping of fiber integrity in healthy aging

Both age groups performed similarly on behavioral measures of interhemispheric transfer (CUD) and integration (RTE) function, albeit with somewhat higher CUDs and RTEs in older than younger adults at a descriptive level. As hypothesized, faster interhemispheric transfer, i.e., smaller CUDs, was related to higher fiber callosal integrity (FA) in anterior but not posterior regions; specifically, to greater genu fiber integrity in younger adults, but greater body fiber integrity in older adults. Also consistent with our hypotheses, faster interhemispheric integration, i.e., greater RTE, was correlated with integrity of subcortical

pontine fiber pathways in older adults. Convergent fMRI evidence showed RTE-related pontine activation that was modulated by response hands and differed between older and younger adults.

The pons is critical for sensory-motor coordination between the two brain hemispheres and links the cerebellum and basal ganglia to motor and sensory cortices and to frontal and prefrontal cortices (Ramnani et al., 2006; Schmahmann and Pandya, 1997). The locus for interhemispheric integration in RTE, that is, the fibers enabling integration between hemispheres, is controversial. Among the systems considered are the corpus callosum (Bucur et al., 2005; Miniussi et al., 1998; Savazzi and Marzi, 2002; Schulte et al., 2006; Turatto et al., 2004), anterior and posterior commissures, subcortical projections through the hippocampal, habenular, and intercollicular brain systems (Aglioti et al., 1996; Corballis, 1998; Corballis et al., 2003; Iaconi et al., 2000; Reuter-Lorenz et al., 1995; Roser and Corballis, 2002, 2003), cerebellar pathways (Glickstein et al., 1998), and pontine tracts (Roser and Corballis, 2002). In support of pontine fiber connectivity for interhemispheric integration, Roser and Corballis (2002) speculated that inputs might proceed via subcortical pathways from the retina to the pons, where they summate and activate the reticular formation, creating an arousal effect that speeds responding. The point-by-point mapping of white matter fiber pathways now showed that response advantages in older adults correlated with FA values in transverse pontine fibers that branch into the right cerebellar cortex, whereas these correlations were not observed in younger adults. The right cerebellar hemisphere is associated with somatomotor (Parsons and Fox, 1997) and visual processing functions (Shulman et al., 1997). Our results are consistent with these structural-functional corticosubcortical pathways in that interhemispheric sensorimotor function was predicted by the integrity of pontine fibers connecting the right cerebellar hemisphere with sensory and motor cortices. Furthermore, our fMRI results showed that the pontine activation cluster extended into the right cerebellum, and the left superior colliculus and thalamus. Considering this together with the second activation cluster in the left medial superior temporal cortex, the observed RTE activation pattern resembles a pathway similar to the cortico-subcortical fiber pathways identified in monkeys going from medial superior temporal cortex to pontine nuclei (Tusa and Ungerleider, 1988). Neural co-activation from redundant targets was further associated with bilateral extrastriate activation, similar to previous fMRI studies that provided evidence for neural co-activation from bilateral redundant targets with enhanced extrastriate activation to bilateral but not unilateral, paired stimulation in young (Schulte et al., 2006) and middle-aged healthy adults (Schulte et al., 2010).

Split-brain studies have demonstrated the relevance of the CC for interhemispheric transfer functions measured with the CUD (Corballis, 1998; Iaconi et al., 2000; Marzi et al., 1991; Mooshagian et al., 2009; Paul et al., 2007; Reuter-Lorenz et al., 1995; Roser and Corballis, 2002). Our study extends these findings to the less dramatic, non-lesion condition of healthy aging by indicating that in older age the integrity of interhemispheric connections affects the efficiency of hemispheric interaction (see also Cherbuin and Brinkman, 2006; Davis et al., 2012). The FTTM analysis has provided a spatially-specific correlation pattern between fiber integrity and CUD with higher FA in left lateral and medial body regions best predicting interhemispheric transfer in older adults. Recently, Langan et al. (2010) found that greater callosal genu size in older adults was associated with more ipsilateral activations of the primary motor cortex during a unimanual motor task and with less intrinsic functional connectivity between left and right motor cortices. Behavioral measures often differ for dominant (right) and nondominant (left) response hands (Derakhshan et al., 2003) (see Fig. 3A). These observations have led to the conclusion that interhemispheric transfer is faster from right to left than from left to right (Barnett and Corballis, 2005; Iwabuchi and Kirk, 2009).

Different factors have been invoked to explain asymmetry in interhemispheric transfer time, such as a smaller average size of right than left occipital lobe resulting in fewer callosal fibers projecting from left-to-right posterior areas (Saron and Davidson, 1989), faster axonal conduction in the right hemisphere relative to the left (Barnett and Corballis, 2005), and different degrees of hemispheric specialization (Nowicka et al., 1996; Rugg and Beaumont, 1978). Callosal fiber integrity may also contribute to functional lateralization (Aboitiz et al., 1992; Häberling et al., 2011; Müller-Oehring et al., 2009). Specifically, genu fiber degradation in older adults may result in the use of alternative routes, for the case herein spatially-specific body fibers, to preserve laterality. Without alternate pathways enabling functional compensation, callosal fiber degradation may simply result in reduced functional laterality of homologous brain regions in the two hemispheres (Fling et al., 2011; Madden et al., 2009) by affecting inhibitory interactions responsible for maintaining hemispheric dominance of particular brain functions (Kinsbourne, 1974). Response facilitation, as occurs with the RTE, may not be subserved by the same mechanisms for left-hand as for right-hand responses, where the bias may be related to white matter hemispheric asymmetry in healthy individuals (Takao et al., 2011). In addition, our RTE-related fMRI findings showed that subcortical pontine activation was modulated by response hand dominance. Visuomotor information transfer and integration may be a bihemispheric event for nondominant motor output, because it may require the participation only of the contralateral cerebral hemisphere for dominant motor output (Derakhshan, 2006; Derakhshan et al., 2003; Hoshiyama and Kakigi, 1999). Consistent with this pattern, our fMRI and DTI data in older adults indicate involvement of the right cerebellar hemisphere– pontine pathway for response facilitation.

Although a link between enhanced RTEs and prolonged CUDs has been suggested in patients with callosal lesions (Iacoboni et al., 2000), behavioral measures of interhemispheric transfer (CUD) and integration (RTE) are normally unrelated in healthy subjects with intact corpora callosa (Zaidel and Iacoboni, 2003). This measurement independence occurred in our younger adults, and a modest relation between greater response facilitation (RTE) and longer interhemispheric transfer times (CUDs) was observed in older adults. In healthy subjects, the CUD value has been estimated, on average, as 4–5 ms (Marzi et al., 1991, 1999), which is about the same time that muscle responses to transcranial stimulation over the left-hand motor cortex can be facilitated when stimulation has been applied 4–5 ms earlier over the right-hand motor cortex (Hanajima et al., 2001). Several studies, however, found highly variable CUDs, including negative CUDs (Bernard et al., 2010; Braun et al., 1996; Marzi et al., 1991; Tettamanti et al., 2002). Explanations for negative CUDs include laterality of motor control (Derakhshan, 2006), hemispheric specialization of attentional components (Mooshagian et al., 2009), and high-speed optimization of both intrahemispheric and interhemispheric dynamics (Braun et al., 2003). Thus, differences in the CUD for left- and right-hand responses may index efficient visuomotor coordination within and between hemispheres that may be interceded by hemispheric dominance (Braun et al., 2003; Derakhshan, 2006). Our study supports this assumption to some extent by showing negative CUDs mainly for right- but not left-hand responses, implying that efficient visuomotor communication requires interhemispheric information exchange for nondominant, but not necessarily for dominant motor output.

## Conclusion

In the face of degrading anterior callosal fibers, older adults appear to use alternative pathways to accomplish visuomotor interhemispheric information transfer and integration for lateralized processing. Instead of showing youthful anterior callosal microstructural-function associations, functional associations of older adults involved medial callosal fiber systems that project to premotor and somatosensory cortices (Hofer and Frahm, 2006), subcortical pontine pathways that connect cerebellar with premotor cortices (Leichnetz et

al., 1984; Schmahmann and Pandya, 1997; Shook et al., 1990), and sensory cortices operating via collicular (May, 2006) and thalamic systems (lateral geniculate nuclei; Schmahmann and Pandya, 1992) to maintain interhemispheric coherence (Teipel et al., 2009). Topographical mapping of fiber tracts via FTTM provides quantitative assessment of focal microstructural integrity at high spatial resolution and enhances our ability to develop maps of functional correlates between selective neuropsychological performance and neuroconnectivity in health and disease.

## Acknowledgments

This work was supported by a National Institute of Aging Grant AG017919, National Institute on Alcohol Abuse and Alcoholism Grants AA018022, AA005965, AA012388, AA017437, and AA017168 and National Institute of Biomedical Imaging and Bioengineering Grant EB008381. We thank Margaret Rosenbloom for critical reading of, and valuable comments on this manuscript.

## References

- Aboitiz F, Scheibel AB, Fisher RS, Zaidel E. Individual differences in brain asymmetries and fiber composition in the human corpus callosum. *Brain Res.* 1992; 598:154–161. [PubMed: 1486478]
- Aglioti S, Smania N, Manfredi M, Berlucchi G. Disownership of left hand and objects related to it in a patient with right brain damage. *Neuroreport.* 1996; 20:293–296. [PubMed: 9051798]
- Barnett KJ, Corballis MC. Speeded right-to-left information transfer: the result of speeded transmission in right-hemisphere axons? *Neurosci Lett.* 2005; 380:88–92. [PubMed: 15854757]
- Bartzokis G, Sultzer D, Lu PH, Nuechterlein KH, Mintz J, Cummings JL. Heterogeneous age-related breakdown of white matter structural integrity: implications for cortical “disconnection” in aging and Alzheimer’s disease. *Neurobiol Aging.* 2004; 25:843–851. [PubMed: 15212838]
- Basser PJ, Pajevic S, Pierpaoli C, Duda J, Aldroubi A. In vivo fiber tractography using DT-MRI data. *Magn Reson Med.* 2000; 44:625–632. [PubMed: 11025519]
- Bennett IJ, Madden DJ, Vaidya CJ, Howard DV, Howard JH Jr. Age-related differences in multiple measures of white matter integrity: a diffusion tensor imaging study of healthy aging. *Hum Brain Mapp.* 2010; 31:378–390. [PubMed: 19662658]
- Bernard JA, Taylor SF, Seidler RD. Handedness, dexterity, and motor cortical representations. *J Neurophysiol.* 2010; 105:88–99. [PubMed: 20943944]
- Bodammer N, Kaufmann J, Kanowski M, Tempelmann C. Eddy current correction in diffusion-weighted imaging using pairs of images acquired with opposite diffusion gradient polarity. *Magn Reson Med.* 2004; 51:188–193. [PubMed: 14705060]
- Braun CMJ, Villeneuve L, Achim A. Balance of cost in interhemispheric relay in the Poffenberger paradigm: evidence from omission errors. *Neuropsychology.* 1996; 10:565–572.
- Braun, CMJ.; Achim, A.; Larocque, C. The Evolution of the Concept of Interhemispheric Relay Time. In: Zaidel, E.; Iacoboni, M., editors. *The Parallel Brain: The Cognitive Neuroscience of the Corpus Callosum.* MIT Press; Cambridge: 2003.
- Bucur B, Madden DJ, Allen PA. Age-related differences in the processing of redundant visual dimensions. *Psychol Aging.* 2005; 20:435–446. [PubMed: 16248703]
- Burzynska AZ, Preuschhof C, Bäckman L, Nyberg L, Li SC, Lindenberger U, Heekeren HR. Age-related differences in white matter microstructure: region-specific patterns of diffusivity. *Neuroimage.* 2010; 49:2104–2112. [PubMed: 19782758]
- Cherbuin N, Brinkman C. Efficiency of callosal transfer and hemispheric interaction. *Neuropsychology.* 2006; 20:178–184. [PubMed: 16594778]
- Corballis MC. Interhemispheric neural summation in the absence of the corpus callosum. *Brain.* 1998; 121:1795–1807. [PubMed: 9762966]
- Corballis MC. Hemispheric interaction in simple reaction time. *Neuropsychologia.* 2002; 40:423–434. [PubMed: 11684175]
- Corballis MC, Corballis PM, Fabri M. Redundancy gain in simple reaction time following partial and complete callosotomy. *Neuropsychologia.* 2003; 42:71–81. [PubMed: 14615077]

- Crovitz HF, Zener K. A group test for assessing hand- and eyedominance. *Am J Psychol.* 1962; 75:271–276. [PubMed: 13882420]
- Davis SW, Kragel JE, Madden DJ, Cabeza R. The architecture of cross-hemispheric communication in the aging brain: linking behavior to functional and structural connectivity. *Cereb Cortex.* 2012; 22:232–242. [PubMed: 21653286]
- de Chastelaine M, Wang TH, Minton B, Muftuler LT, Rugg MD. The effects of age, memory performance, and callosal integrity on the neural correlates of successful associative encoding. *Cereb Cortex.* 2011; 21:2166–2176. [PubMed: 21282317]
- Derakhshan I. Crossed-uncrossed difference (CUD) in a new light: anatomy of the negative CUD in Poffenberger's paradigm. *Acta Neurol Scand.* 2006; 113:203–208. [PubMed: 16441252]
- Derakhshan I, Franz EA, Rowse A. An exchange on Franz, Rowse, and Ballantine (2002) Handedness, neural versus behavioral: is there a measureable callosal difference. *J Mot Behav.* 2003; 35:409–414. [PubMed: 14607777]
- Douaud G, Jbabdi S, Behrens TE, Menke RA, Gass A, Monsch AU, Rao A, Whitcher B, Kindlmann G, Matthews PM, Smith S. DTI measures in crossing-fibre areas: increased diffusion anisotropy reveals early white matter alteration in MCI and mild Alzheimer's disease. *Neuroimage.* 2011; 55:880–890. [PubMed: 21182970]
- Fedorov A, Beichel R, Kalpathy-Cramer J, Finet J, Fillion-Robin JC, Pujol S, Bauer C, Jennings D, Fennessy F, Sonka M, Buatti J, Aylward S, Miller JV, Pieper S, Kikinis R. 3D slicer as an image computing platform for the Quantitative Imaging Network. *Magn Reson Imaging.* 2012; 30:1323–1341. [PubMed: 22770690]
- Fling BW, Seidler RD. Fundamental differences in callosal structure, neuro-physiologic function, and bimanual control in young and older adults. *Cereb Cortex.* 2011 Dec 12.
- Fling BW, Walsh CM, Bangert AS, Reuter-Lorenz PA, Welsh RC, Seidler RD. Differential callosal contributions to bimanual control in young and older adults. *J Cogn Neurosci.* 2011; 23:2171–2185. [PubMed: 20954936]
- Friston KJ, Frith CD, Frackowiak RS, Turner R. Characterizing dynamic brain responses with fMRI: a multivariate approach. *Neuroimage.* 1995a; 2:166–172. [PubMed: 9343599]
- Friston KJ, Frith CD, Turner R, Frackowiak RS. Characterizing evoked hemodynamics with fMRI. *Neuroimage.* 1995b; 2:157–165. [PubMed: 9343598]
- Genç E, Bergmann J, Tong F, Blake R, Singer W, Kohler A. Callosal connections of primary visual cortex predict the spatial spreading of binocular rivalry across the visual hemifields. *Front Hum Neurosci.* 2011; 5:161. [PubMed: 22162968]
- Genovese CR, Lazar NA, Nichols T. Thresholding of statistical maps in functional neuroimaging using the false discovery rate. *Neuroimage.* 2002; 15:870–878. [PubMed: 11906227]
- Glickstein M, Buchbinder S, May JL III. Visual control of the arm, the wrist and the fingers: pathways through the brain. *Neuropsychologia.* 1998; 36:981–1001. [PubMed: 9845046]
- Gooijers, J.; Caeyenberghs, K.; Sisti, HM.; Geurts, M.; Heitger, MH.; Leemans, A.; Swinnen, SP. Diffusion tensor imaging metrics of the corpus callosum in relation to bimanual coordination: effect of task complexity and sensory feedback. *Hum Brain Mapp.* 2011. <http://dx.doi.org/10.1002/hbm.21429> (Epub ahead of print)
- Häberling IS, Badzakova-Trajkov G, Corballis MC. Callosal tracts and patterns of hemispheric dominance: a combined fMRI and DTI study. *Neuroimage.* 2011; 54:779–786. [PubMed: 20920586]
- Hanajima R, Ugawa Y, Machii K, Mochizuki H, Terao Y, Enomoto H, Furubayashi T, Shiio Y, Uesugi H, Kanazawa I. Interhemispheric facilitation of the hand motor area in humans. *J Physiol.* 2001; 531:849–859. [PubMed: 11251064]
- Hofer S, Frahm J. Topography of the human corpus callosum revisited—comprehensive fiber tractography using diffusion tensor magnetic resonance imaging. *Neuroimage.* 2006; 32:989–994. [PubMed: 16854598]
- Hollingshead, AB.; Redlich, FC. *Social Class and Mental Illness: a Community Survey.* John Wiley & Sons; New York: 1958.
- Hoptman MJ, Davidson RJ, Gudmundsson A, Schreiber RT, Ershler WR. Age-difference in visual evoked potential estimates of interhemispheric transfer. *Neuropsychology.* 1996; 10:263–271.

- Hoshiyama M, Kakigi R. Changes of somatosensory evoked potentials during writing with the dominant and non-dominant hands. *Brain Res.* 1999; 833:10–19. [PubMed: 10375672]
- Hou J, Pakkenberg B. Age-related degeneration of corpus callosum in the 90+ years measured with stereology. *Neurobiol Aging.* 2011 Nov 25.
- Iacoboni M, Zaidel E. Interhemispheric visuo-motor integration in humans: the effect of redundant targets. *Eur J Neurosci.* 2003; 17:1981–1986. [PubMed: 12752798]
- Iacoboni M, Ptito A, Weekes NY, Zaidel E. Parallel visuomotor processing in the split brain: cortico-subcortical interactions. *Brain.* 2000; 123:759–769. [PubMed: 10734007]
- Iwabuchi SJ, Kirk IJ. Atypical interhemispheric communication in left-handed individuals. *Neuroreport.* 2009; 20:166–169. [PubMed: 19104458]
- Jeeves MA, Moes P. Interhemispheric transfer time differences related to aging and gender. *Neuropsychologia.* 1996; 34:627–636. [PubMed: 8783215]
- Jenkinson M. A fast, automated, N-dimensional phase unwrapping algorithm. *J Magn Reson Med.* 2003; 49:193–197.
- Jones, DK. *Diffusion MRI: Theory, Methods, and Applications.* Oxford University Press; USA: 2010.
- Kinsbourne, M. Mechanisms of hemispheric interaction in the brain. In: Kinsbourne, M.; Smith, WL., editors. *Hemispheric Disconnection and Cerebral Function.* Thomas; Springfield: 1974. p. 260-285.
- Langan J, Peltier SJ, Bo J, Fling BW, Welsh RC, Seidler RD. Functional implications of age differences in motor system connectivity. *Front Syst Neurosci.* 2010; 4:17. [PubMed: 20589101]
- Leichnetz GR, Smith DJ, Spencer RF. Cortical projections to the paramedian tegmental and basilar pons in the monkey. *J Comp Neurol.* 1984; 228:388–408. [PubMed: 6480918]
- Linnert E, Roser ME. Age-related differences in interhemispheric visuomotor integration measured by the redundant target effect. *Psychol Aging.* 2012; 2:399–409. [PubMed: 21843007]
- Lu PH, Lee GJ, Tishler TA, Meghpara M, Thompson PM, Bartzokis G. Myelin breakdown mediates age-related slowing in cognitive processing speed in healthy elderly men. *Brain Cogn.* 2012; 81:131–138. [PubMed: 23195704]
- Maddah M, Grimson WE, Warfield SK, Wells WM. A unified framework for clustering and quantitative analysis of white matter fiber tracts. *Med Image Anal.* 2008; 12:191–202. [PubMed: 18180197]
- Maddah M, Miller JV, Sullivan EV, Pfefferbaum A, Rohlfing T. Sheet-like white matter fiber tracts: representation, clustering, and quantitative analysis. *Med Image Comput Comput Assist Interv.* 2011; 14:191–199. [PubMed: 21995029]
- Madden DJ, Whiting WL, Huettel SA, White LE, MacFall JR, Provenzale JM. Diffusion tensor imaging of adult age differences in cerebral white matter: relation to response time. *Neuroimage.* 2004; 21:1174–1181. [PubMed: 15006684]
- Madden DJ, Bennett IJ, Song AW. Cerebral white matter integrity and cognitive aging: contributions from diffusion tensor imaging. *Neuropsychol Rev.* 2009; 19:415–435. [PubMed: 19705281]
- Maertens M, Pollmann S. Interhemispheric resource sharing: decreasing benefits with increasing processing efficiency. *Brain Cogn.* 2005; 58:183–192. [PubMed: 15919550]
- Marchand WR, Lee JN, Suchy Y, Garn C, Johnson S, Wood N, Chelune G. Age-related changes of the functional architecture of the cortico-basal ganglia circuitry during motor task execution. *Neuroimage.* 2011; 55:194–203. [PubMed: 21167945]
- Marks NL, Hellige JB. Interhemispheric interaction in bilateral redundancy gain: effects of stimulus format. *Neuropsychology.* 2003; 17:578–593. [PubMed: 14599271]
- Marzi CA, Bisiacchi P, Nicoletti R. Is interhemispheric transfer of visuomotor information asymmetric? Evidence from a meta-analysis. *Neuropsychologia.* 1991; 29:1163–1177. [PubMed: 1838793]
- Marzi CA, Perani D, Tasinari G, Colleluori A, Maravita A, Miniussi C, Paulesu E, Scifo P, Fazio F. Pathways of interhemispheric transfer in normals and in a split-brain subject. A positron emission tomography study. *Exp Brain Res.* 1999; 126:451–458. [PubMed: 10422707]
- May PJ. The mammalian superior colliculus: laminar structure and connections. *Prog Brain Res.* 2006; 151:321–378. [PubMed: 16221594]

- Miller J. Divided attention: evidence for coactivation with redundant signals. *Cogn Psychol.* 1982; 14:247–279. [PubMed: 7083803]
- Miller J. Time course of coactivation in bimodal divided attention. *Percept Psychophys.* 1986; 40:331–343. [PubMed: 3786102]
- Miniussi C, Girelli M, Marzi CA. Neural site of the redundant target effect electrophysiological evidence. *J Cogn Neurosci.* 1998; 10:216–230. [PubMed: 9555108]
- Mooshagian E, Iacoboni M, Zaidel E. Spatial attention and interhemispheric visuomotor integration in the absence of the corpus callosum. *Neuropsychologia.* 2009; 47:933–937. [PubMed: 19124029]
- Mordkoff JT, Yantis S. An interactive race model of divided attention. *J Exp Psychol Hum Percept Perform.* 1991; 17:520–538. [PubMed: 1830090]
- Mori S, Oishi K, Jiang H, Jiang L, Li X, Akhter K, Hua K, Faria AV, Mahmood A, Woods R, Toga AW, Pike GB, Neto PR, Evans A, Zhang J, Huang H, Miller MI, van Zijl P, Mazziotta J. Stereotaxic white matter atlas based on diffusion tensor imaging in an ICBM template. *Neuroimage.* 2008; 40:570–582. [PubMed: 18255316]
- Muetzel RL, Collins PF, Mueller BA, Schissel A, Lim KO, Luciana M. The development of corpus callosum microstructure and associations with bimanual task performance in healthy adolescents. *Neuroimage.* 2008; 39:1918–1925. [PubMed: 18060810]
- Müller-Oehring EM, Schulte T, Fama R, Pfefferbaum A, Sullivan EV. Global–local interference is related to callosal compromise in alcoholism: a behavior-DTI association study. *Alcohol Clin Exp Res.* 2009; 33:477–489. [PubMed: 19120053]
- Neeman M, Freyer JP, Sillerud LO. A simple method for obtaining cross-term-free images for diffusion anisotropy studies in NMR microimaging. *Magn Reson Med.* 1991; 21:138–143. [PubMed: 1943671]
- Nelson, HE. National Adult Heading Test (NART): Test Manual. NFER-Nelson; Windsor: 1982.
- Nowicka A, Grabowska A, Fersten E. Interhemispheric transmission of information and functional asymmetry of the human brain. *Neuropsychologia.* 1996; 34:147–151. [PubMed: 8852877]
- O'Sullivan M, Jones DK, Summers PE, Morris RG, Williams SC, Markus HS. Evidence for cortical “disconnection” as a mechanism of age-related cognitive decline. *Neurology.* 2001; 57:632–638. [PubMed: 11524471]
- Parsons, LM.; Fox, PT. Section IV: Functional neuroimaging studies. Sensory and cognitive functions. In: Schmahmann, JD., editor. *The cerebellum and cognition* *Int Rev Neurobiol.* Vol. 41. 1997. p. 255-272.
- Paul LK, Brown WS, Adolphs R, Tyszka JM, Richards LJ, Mukherjee P, Sherr EH. Agenesis of the corpus callosum: genetic, developmental and functional aspects of connectivity. *Nat Rev Neurosci.* 2007; 8:287–299. [PubMed: 17375041]
- Pfefferbaum A, Sullivan EV. Increased brain white matter diffusivity in normal adult aging: relationship to anisotropy and partial voluming. *Magn Reson Med.* 2003; 49:953–961. [PubMed: 12704779]
- Pfefferbaum A, Sullivan EV, Hedehus M, Lim KO, Adalsteinsson E, Moseley M. Age-related decline in brain white matter anisotropy measured with spatially corrected echo-planar diffusion tensor imaging. *Magn Reson Med.* 2000; 44:259–268. [PubMed: 10918325]
- Pfefferbaum A, Adalsteinsson E, Sullivan EV. Frontal circuitry degradation marks healthy adult aging: evidence from diffusion tensor imaging. *Neuroimage.* 2005; 26:891–899. [PubMed: 15955499]
- Pierpaoli C, Basser PJ. Towards a quantitative assessment of diffusion anisotropy. *Magn Reson Med.* 1996; 36:893–906. [PubMed: 8946355]
- Poffenberger AT. Reaction time to retinal stimulation with special reference to time lost in conduction through nerves center. *Arch Psychol.* 1912; 23:1–173.
- Poline JB, Worsley KJ, Evans AC, Friston KJ. Combining spatial extent and peak intensity to test for activations in functional imaging. *Neuroimage.* 1997; 5:83–96. [PubMed: 9345540]
- Pollmann S, Zaidel E. Redundancy gains for visual search after complete commissurotomy. *Neuropsychology.* 1999; 13:246–258. [PubMed: 10353374]
- Raab DH. Statistical facilitation of simple reaction times. *Trans N Y Acad Sci.* 1962; 24:574–590. [PubMed: 14489538]

- Ramnani N, Behrens TE, Johansen-Berg H, Richter MC, Pinsk MA, Andersson JL, Rudebeck P, Ciccarelli O, Richter W, Thompson AJ, Gross CG, Robson MD, Kastner S, Matthews PM. The evolution of prefrontal inputs to the corticopontine system: diffusion imaging evidence from Macaque monkeys and humans. *Cereb Cortex*. 2006; 16:811–818. [PubMed: 16120793]
- Raz N, Ghisletta P, Rodrigue KM, Kennedy KM, Lindenberger U. Trajectories of brain aging in middle-aged and older adults: regional and individual differences. *Neuroimage*. 2010; 51:501–511. [PubMed: 20298790]
- Reuter-Lorenz PA, Stanczak L. Differential effects of aging on the functions of the corpus callosum. *Dev Neuropsychol*. 2000; 18:113–137. [PubMed: 11143802]
- Reuter-Lorenz PA, Nozawa G, Gazzaniga MS, Hughes HC. Fate of neglected targets: a chronometric analysis of redundant target effects in the bisected brain. *J Exp Psychol Hum Percept Perform*. 1995; 21:211–230. [PubMed: 7714469]
- Rohlfing R. Incorrect ICBM-DTI-81 atlas orientation and white matter labels. *Front Neurosci*. 2013; 7 Epub 2013 Jan 25.
- Roser M, Corballis MC. Interhemispheric neural summation in the split brain with symmetrical and asymmetrical displays. *Neuropsychologia*. 2002; 40:1300–1312. [PubMed: 11931933]
- Roser M, Corballis MC. Interhemispheric neural summation in the split brain: effects of stimulus colour and task. *Neuropsychologia*. 2003; 41:830–846. [PubMed: 12631533]
- Rugg MD, Beaumont JG. Interhemispheric asymmetries in the visual evoked response: effects of stimulus lateralisation and task. *Biol Psychol*. 1978; 6:283–292. [PubMed: 708813]
- Salat DH, Tuch DS, Greve DN, van der Kouwe AJ, Hevelone ND, Zaleta AK, Rosen BR, Fischl B, Corkin S, Rosas HD, Dale AM. Age-related alterations in white matter microstructure measured by diffusion tensor imaging. *Neurobiol Aging*. 2005; 26:1215–1227. [PubMed: 15917106]
- Saltzberg B, Burton WD Jr, Burch NR, Fletcher J, Michaels R. Electrophysiological measures of regional neural interactive coupling. Linear and non-linear dependence relationships among multiple channel electroencephalographic recordings. *Int J Biomed Comput*. 1986; 18:77–87. [PubMed: 3699920]
- Saron CD, Davidson RJ. Visual evoked potential measures of interhemispheric transfer time in humans. *Behav Neurosci*. 1989; 103:1115–1138. [PubMed: 2803556]
- Savazzi S, Marzi CA. Speeding up reaction time with invisible stimuli. *Curr Biol*. 2002; 12:403–407. [PubMed: 11882292]
- Savazzi S, Marzi CA. The superior colliculus subserves interhemispheric neural summation in both normals and patients with a total section or agenesis of the corpus callosum. *Neuropsychologia*. 2004; 42:1608–1618. [PubMed: 15327929]
- Schmahmann JD, Pandya DN. Course of the fiber pathways to pons from parasensory association areas in the rhesus monkey. *J Comp Neurol*. 1992; 326:159–179. [PubMed: 1479073]
- Schmahmann JD, Pandya DN. Anatomic organization of the basilar pontine projections from prefrontal cortices in rhesus monkey. *J Neurosci*. 1997; 17:438–458. [PubMed: 8987769]
- Schulte T, Müller-Oehring EM. Contribution of callosal connections to the interhemispheric integration of visuomotor and cognitive processes. *Neuropsychol Rev*. 2010; 20:174–190. [PubMed: 20411431]
- Schulte T, Pfefferbaum A, Sullivan EV. Parallel interhemispheric processing in aging and alcoholism: relation to corpus callosum size. *Neuropsychologia*. 2004; 42:257–271. [PubMed: 14644111]
- Schulte T, Sullivan EV, Müller-Oehring EM, Adalsteinsson E, Pfefferbaum A. Corpus callosal microstructural integrity influences interhemispheric processing: a diffusion tensor imaging study. *Cereb Cortex*. 2005; 15:1384–1392. [PubMed: 15635059]
- Schulte T, Chen SH, Müller-Oehring EM, Adalsteinsson E, Pfefferbaum A, Sullivan EV. fMRI evidence for individual differences in premotor modulation of extrastriatal visual–perceptual processing of redundant targets. *Neuroimage*. 2006; 30:973–982. [PubMed: 16356737]
- Schulte T, Müller-Oehring EM, Rohlfing T, Pfefferbaum A, Sullivan EV. White matter fiber degradation attenuates hemispheric asymmetry when integrating visuomotor information. *J Neurosci*. 2010; 30:12168–12178. [PubMed: 20826679]

- Shook L, Schlag-Rey M, Schlag J. Primate supplementary eye field. I. Comparative aspects of mesencephalic and pontine connections. *J Comp Neurol.* 1990; 301:618–642. [PubMed: 2273101]
- Shulman GL, Corbetta M, Buckner RL, Fiez JA, Miezin FM, Raichle ME, Petersen SE. Common blood flow changes across visual tasks: I. Increases in subcortical structures and the cerebellum but not in nonvisual cortex. *J Cogn Neurosci.* 1997; 9:624–647. [PubMed: 23965121]
- Smith SM, Jenkinson H, Johansen-Berg H, Rueckert D, Nichols TE, Mackay CE, Watkins KW, Ciccarelli O, Cader MZ, Matthews PM, Behrens TEJ. Tract-based spatial statistics: voxelwise analysis of multi-subject diffusion data. *Neuroimage.* 2006; 31:1487–1505. [PubMed: 16624579]
- Stadlbauer A, Salomonowitz E, Strunk G, Hammen T, Ganslandt O. Age-related degradation in the central nervous system: assessment with diffusion-tensor imaging and quantitative fiber tracking. *Radiology.* 2008; 247:179–188. [PubMed: 18292477]
- Sullivan EV, Adalsteinsson E, Pfefferbaum A. Selective age-related degradation of anterior callosal fiber bundles quantified in vivo with fiber tracking. *Cereb Cortex.* 2006; 16:1030–1039. [PubMed: 16207932]
- Sullivan EV, Rohlfing T, Pfefferbaum A. Quantitative fiber tracking of lateral and interhemispheric white matter systems in normal aging: relations to timed performance. *Neurobiol Aging.* 2010; 31:464–481. [PubMed: 18495300]
- Takao H, Hayashi N, Ohtomo K. White matter asymmetry in healthy individuals: a diffusion tensor imaging study using tract-based spatial statistics. *Neuroscience.* 2011; 193:291–299. [PubMed: 21824507]
- Teipel SJ, Pogarell O, Meindl T, Dietrich O, Sydykova D, Hunklinger U, Georgii B, Mulert C, Reiser MF, Möller HJ, Hampel H. Regional networks underlying interhemispheric connectivity: an EEG and DTI study in healthy ageing and amnesic mild cognitive impairment. *Hum Brain Mapp.* 2009; 30:2098–2119. [PubMed: 18781594]
- Tettamanti M, Paulesu E, Scifo P, Maravita A, Fazio F, Perani D, Marzi CA. Interhemispheric transmission of visuomotor information in humans: fMRI evidence. *J Neurophysiol.* 2002; 88:1051–1058. [PubMed: 12163553]
- Turatto M, Mazza V, Savazzi S, Marzi CA. The role of the magnocellular and parvocellular systems in the redundant target effect. *Exp Brain Res.* 2004; 158:141–150. [PubMed: 15007588]
- Tusa RJ, Ungerleider LG. Fiber pathways of cortical areas mediating smooth pursuit eye movements in monkeys. *Ann Neurol.* 1988; 23:174–183. [PubMed: 3288083]
- Walker, H.; Lev, J. *Statistical Inference.* Holt; New York, NY: 1953.
- Wolf, D.; Fischer, FU.; Fesenbeckh, J.; Yakushev, I.; Lelieveld, IM.; Scheurich, A.; Schermuly, I.; Zschutschke, L.; Fellgiebel, A. Structural integrity of the corpus callosum predicts long-term transfer of fluid intelligence-related training gains in normal aging. *Hum Brain Mapp.* 2012. <http://dx.doi.org/10.1002/hbm.22177> (Epub ahead of print)
- Zahr NM, Rohlfing T, Pfefferbaum A, Sullivan EV. Problem solving, working memory, and motor correlates of association and commissural fiber bundles in normal aging: a quantitative fiber tracking study. *Neuroimage.* 2009; 44:1050–1062. [PubMed: 18977450]
- Zaidel, E.; Iacoboni, M. Poffenberger's simple reaction time paradigm for measuring interhemispheric transfer time. In: Zaidel, E.; Iacoboni, M., editors. *The parallel brain.* MIT; Cambridge: 2003. p. 1-8.

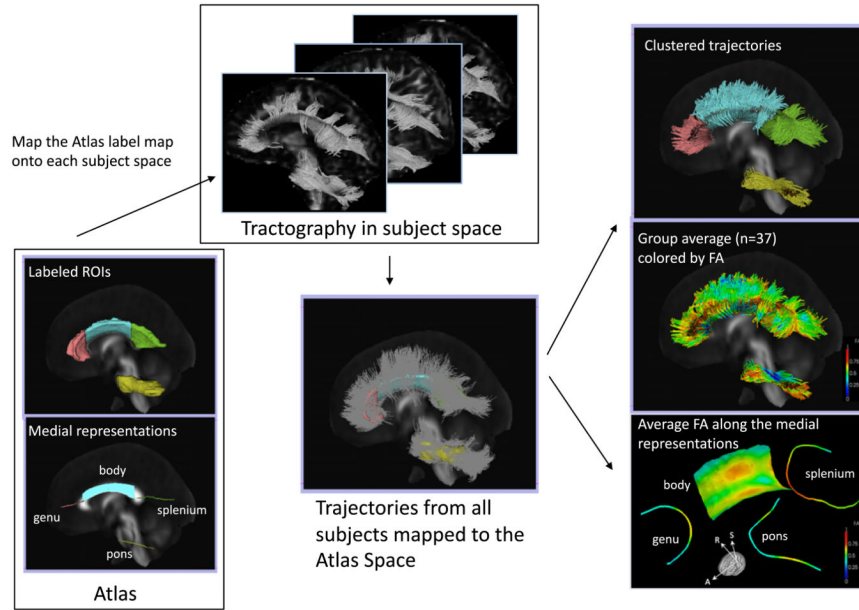


**Fig. 1.** Pipeline for DTI-based fiber tract-driven topographic mapping (FTTM) analysis. Left panel: (Bottom) Labeled ROIs in the ICBM-DTI-81 atlas and the derived initial medial representation of each bundle. Middle panel: (Top) The ROIs are mapped to each subject space by applying the affine transformation obtained by registering the FA volume of the atlas to the FA volume of each subject. Seeded from the registered ROIs, streamline tractography is performed in each subject's native image space. (Bottom) Trajectories from all 37 subjects are mapped back to the atlas space and are clustered into bundles based on their spatial proximity and shape similarity to the medial representation of fiber tracts in the atlas. Right panel: (Top) Trajectories are colored with the most probable label assigned in the clustering process. (Middle) Trajectories are colored with the FA values. (Bottom) The medial representation of each bundle is colored by the average FA of trajectories in each bundle summarizing the local variation of the diffusion parameter along that fiber bundle, thereby providing topographic parameter maps.

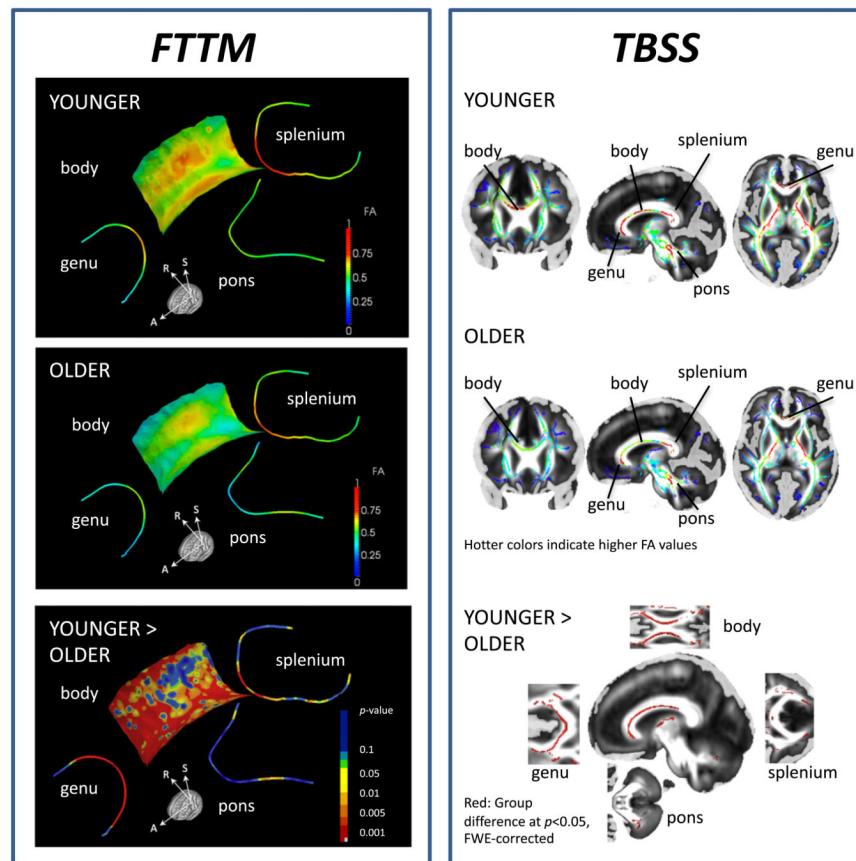


**Fig. 2.** Interhemispheric white matter fiber integrity maps. Left: FTTM-derived FA maps for callosal fiber tracts (genu, body, and splenium), and for pontine fiber tracts in younger (top) and older adults (middle). FTTM-derived  $p$ -value map (bottom) illustrating spatially-specific group differences (younger > older) in FA projected onto average-FA skeleton for callosal (genu, body, splenium) and pontine fiber tracts. Right: TBSS-derived FA maps for older (top) and younger adults (middle); and group difference map (bottom) for FA younger > older adults ( $p_{\text{FWE corrected}} = 0.05$ ).

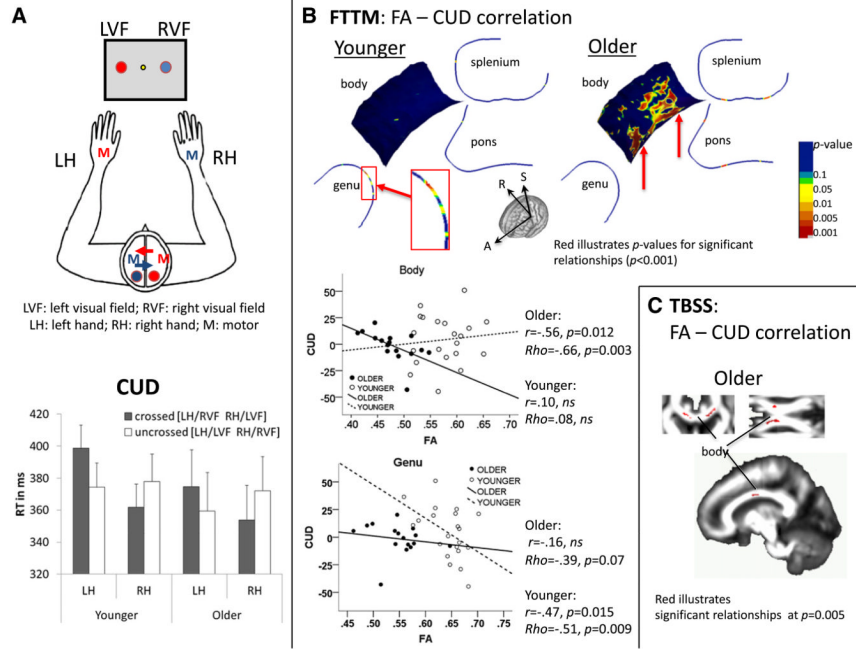


**Fig. 3.** Interhemispheric fiber integrity and interhemispheric transfer function — crossed–uncrossed difference (CUD). A. Illustration of left visual field (LVF) and right visual field (RVF) stimulation and left-hand (LH) and right-hand (RH) responses requiring interhemispheric information transfer for crossed (LVF/RH; RVF/LH) in contrast to uncrossed conditions (LVF/LH; RVF/RH); and mean reaction times (standard error) for crossed and uncrossed conditions differentiated for LH and RH responses for younger and older adults. B. FTMM-derived correlation map between CUD and body FA in older adults; and correlation scatter plots illustrating the correlation between CUD and the averaged FA value for regional callosal and pontine fiber bundles in younger and older adults. C. TBSS-derived correlation map between CUD and body FA in older adults.

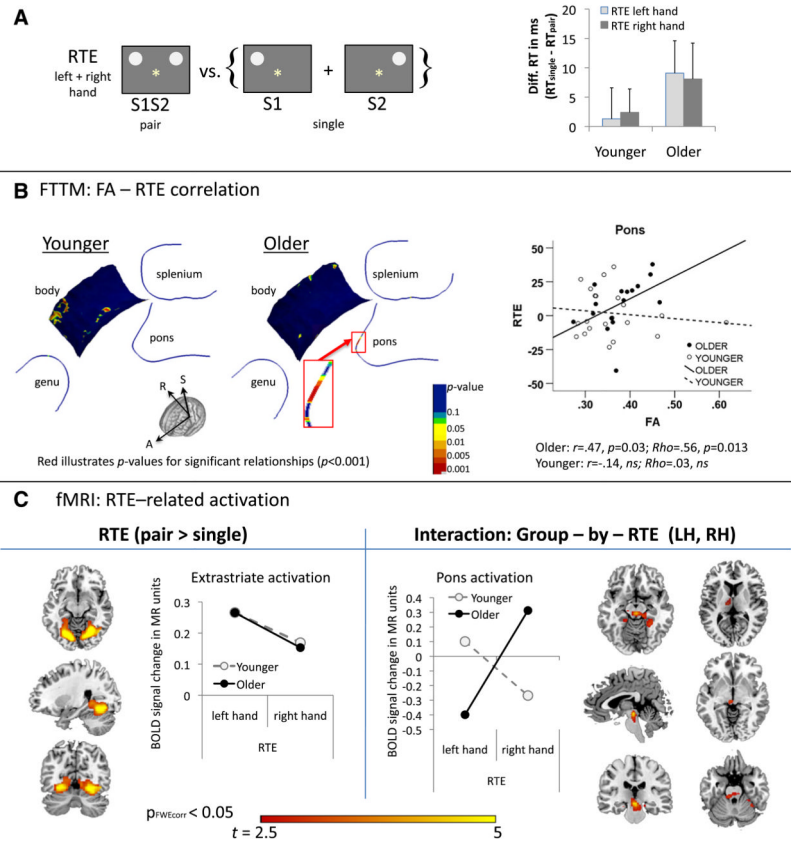


**Fig. 4.** Interhemispheric fiber integrity and interhemispheric integration — redundant targets effects (RTE). A. RTE was calculated as the difference in reaction time between paired (S1S2) and single (S1, S2) stimulation conditions: Means (standard errors) for LH and RH responses in younger and older adults. B. FTSM-derived correlation map illustrating significant relationships between interhemispheric facilitation (RTE) and fiber integrity (FA) along the pontine fiber tract in older adults. Graphs illustrate the correlation between RTE for right hand responses and averaged FA of the right branch pontine fiber tract in younger and older adults. C. fMRI activation for RTE (pair > single), including group (older, younger) and response hand (left, right) as factors, revealed bilateral extrastriate activation, and a 2-way interaction (group-by-RTE response hand) revealed a subcortical pontine activation cluster. Graphs illustrate RTE-related BOLD signal changes (pair > single) for response hand and group. The  $p$ -threshold was set at  $p_{FWECorr} = 0.05$  for combined spatial extent and peak intensity thresholds (Poline et al., 1997).

**Table 1**

Demographic data of the two groups: mean (standard deviation).

Group	Men/women	Age	Education	SES <sup>a</sup>	ANART IQ <sup>b</sup>	Handedness <sup>c</sup>
Younger	11/10	24 (19–30)	16 (1.2)	26 (10.3)	113 (7.9)	19 (3.9)
Older	9/7	72 (60–85)	17 (2.4)	20 (10.1)	122 (6.1)	18 (4.0)
<i>p</i>	<i>ns</i>	.0001	<i>ns</i>	.06	.005	<i>ns</i>

<sup>a</sup>Lower scores are in the direction of higher socioeconomic status (SES).

<sup>b</sup>American National Adult Reading Test Intelligence Quotient.

<sup>c</sup>Handedness questionnaire scores 14–32 index right-handedness, scores 50–70 left-handedness, and scores 33–49 ambidexterity (Crovitz and Zener, 1962).

**Table 2**

Behavioral performance of younger and older healthy adults.

	Left hand		RTE-LH		Right hand		RTE-RH		CUD	RTE
	LVF	RVF	PAIR	RVF	LVF	RVF	PAIR			
Younger	378.6 (62.8)	398.6 (67)	387.3 (69.9)	1.31 (24.3)	361.9 (66.4)	377.9 (78.9)	367.2 (75.5)	2.39 (18.2)	4.17 (23.2)	1.85 (16.9)
Older	359.5 (96.8)	374.7 (92.7)	358.9 (100.3)	9.08 (21.8)	353.9 (86.5)	372 (85.9)	354.9 (98.1)	8.06 (24.4)	-1.46 (14.2)	8.57 (18.7)

Mean reaction time (standard deviation) in milliseconds to single left (LVF), single right (RVF), and paired bilateral (PAIR) visual field stimulation for left (LH) and right hand (RH) responses. RTE = redundant targets effect; CUD = crossed-uncrossed difference.

Table 3

RTE-related brain activation and group interaction.

Brain region	Cluster		MNI coordinates		
	<i>k</i>	<i>T</i>	<i>x</i>	<i>y</i>	<i>z</i>
<i>RTE</i>					
Bilateral extrastriate cortices	4242	6.92	28	-60	-12
		5.83	22	-70	-10
		5.74	-16	-76	-10
<i>Interaction: Group-by-RTE response hand</i>					
Bilateral pons	1115	4.87	0	-26	-12
			-10	-18	6
			-12	-32	-20
Left medial superior temporal cortex/insula <sup>a</sup>	972	4.34	-46	6	-10
			-40	12	-24

RTE = redundant targets effect; contrast of interest: pair (S1S2) > single (S1 + S2); Interaction: Older > Younger for RTE-RH > RTE-LH; statistical threshold was set at  $p_{FWecorr} < 0.05$  for combined spatial extent and peak intensity (Poline et al., 1997).

<sup>a</sup>  $p_{FDRcorr} = 0.029$ ;  $p_{FWecorr} = 0.067$ .